




MbnC Is Not Required for the Formation of the N-Terminal Oxazolone in the Methanobactin from *Methylosinus trichosporium* OB3b

Philip Dershwitz,^a Wenyu Gu,^{b*} Julien Roche,^a Christina S. Kang-Yun,^{b,§}  Jeremy D. Semrau,^b Thomas A. Bobik,^a Bruce Fulton,^a Hans Zischka,^{c,d}  Alan A. DiSpirito^a

^aRoy J. Carver Department of Biochemistry, Biophysics and Molecular Biology, Iowa State University, Ames, Iowa, USA

^bDepartment of Civil and Environmental Engineering, University of Michigan, Ann Arbor, Michigan, USA

^cInstitute of Molecular Toxicology and Pharmacology, Helmholtz Center Munich, German Research Center for Environmental Health, Neuherberg, Germany

^dTechnical University München, School of Medicine, Institute of Toxicology and Environmental Hygiene, Munich, Germany

Philip Dershwitz and Wenyu Gu are co-first authors. Both P. Dershwitz and W. Gu made similar contributions to the manuscript, with W. Gu responsible for all of the molecular cloning and genetic characterization of the *mbnG* minus mutant, while P. Dershwitz isolated and structurally characterized the *mbnG* mutant. Both contributions were major to the development of the project. However, the authors decided that the effort required for the structural characterization of MbnC was more than the genetic characterization, so the order is P. Dershwitz first and W. Gu second.

ABSTRACT Methanobactins (MBs) are ribosomally synthesized and posttranslationally modified peptides (RiPPs) produced by methanotrophs for copper uptake. The posttranslational modification that defines MBs is the formation of two heterocyclic groups with associated thioamines from X-Cys dipeptide sequences. Both heterocyclic groups in the MB from *Methylosinus trichosporium* OB3b (MB-OB3b) are oxazolone groups. The precursor gene for MB-OB3b is *mbnA*, which is part of a gene cluster that contains both annotated and unannotated genes. One of those unannotated genes, *mbnC*, is found in all MB operons and, in conjunction with *mbnB*, is reported to be involved in the formation of both heterocyclic groups in all MBs. To determine the function of *mbnC*, a deletion mutation was constructed in *M. trichosporium* OB3b, and the MB produced from the Δ *mbnC* mutant was purified and structurally characterized by UV-visible absorption spectroscopy, mass spectrometry, and solution nuclear magnetic resonance (NMR) spectroscopy. MB-OB3b from the Δ *mbnC* mutant was missing the C-terminal Met and was also found to contain a Pro and a Cys in place of the pyrrolidinyl-oxazolone-thioamide group. These results demonstrate MbnC is required for the formation of the C-terminal pyrrolidinyl-oxazolone-thioamide group from the Pro-Cys dipeptide, but not for the formation of the N-terminal 3-methylbutanol-oxazolone-thioamide group from the N-terminal dipeptide Leu-Cys.

IMPORTANCE A number of environmental and medical applications have been proposed for MBs, including bioremediation of toxic metals and nanoparticle formation, as well as the treatment of copper- and iron-related diseases. However, before MBs can be modified and optimized for any specific application, the biosynthetic pathway for MB production must be defined. The discovery that *mbnC* is involved in the formation of the C-terminal oxazolone group with associated thioamide but not for the formation of the N-terminal oxazolone group with associated thioamide in *M. trichosporium* OB3b suggests the enzymes responsible for posttranslational modification(s) of the two oxazolone groups are not identical.

KEYWORDS methanobactin, chalkophore, methanotroph, aerobic methane oxidation, ribosomally synthesized and posttranslational modified peptide

Methanobactins (MBs) are low-molecular-mass (<1,300 Da), posttranslationally modified copper-binding peptides excreted by some methanotrophs as the extracellular component of a copper acquisition system (1–7). Structurally MBs are

Editor Robert M. Kelly, North Carolina State University

Copyright © 2022 Dershwitz et al. This is an open-access article distributed under the terms of the [Creative Commons Attribution 4.0 International license](https://creativecommons.org/licenses/by/4.0/).

Address correspondence to Alan A. DiSpirito, aland@iastate.edu.

*Present address: Wenyu Gu, Department of Civil & Environmental Engineering, Stanford University, Stanford, California, USA.

§Present address: Christina S. Kang-Yun, Biosciences and Biotechnology Division, Lawrence Livermore National Laboratory, Livermore, California, USA.

Received 15 September 2021

Accepted 31 October 2021

Accepted manuscript posted online

3 November 2021

Published 25 January 2022

characterized by the presence of a C-terminal oxazolone group with a C2-associated thioamide and by the presence of an N-terminal oxazolone, imidazolone or pyrazinedione group with an associated thioamide. Some MBs also contain a sulfate group in place of the hydroxyl group on a Tyr adjacent to the C-terminal oxazolone group. The best-characterized MB is from *Methylophilus trichosporium* OB3b (MB-OB3b), and the posttranslational modifications for this MB involve (i) deamination of the N-terminal Leu, (ii) conversion of the N-terminal Leu-Cys dipeptide to 1-(N-(mercapto-(5-oxo-2-(3-methylbutanoyl)oxazol-(Z)-4-ylidene)methyl)), (iii) conversion of the C-terminal Pro-Cys dipeptide into pyrrolidin-2-yl-(mercapto-(5-oxo-oxazol-(Z)-4-ylidene)methyl), and (iv) cleavage of the leader sequence (2, 4, 5, 8–11).

The gene encoding the MB precursor peptide, *mbnA* (5, 10), is found in a gene cluster that contains both genes of known function, such as *mbnB* (5, 11), *mbnN* (9), and *mbnT* (12), as well as unannotated genes, such as *mbnC* (5, 10, 11, 13, 14). MbnB is a member of TIM barrel family as well as the DUF692 family of diiron enzymes (11, 14). In heterologous expression studies in *Escherichia coli*, MbnBC was shown to catalyze a dioxygen-dependent four-electron oxidation of Pro-Cys in MbnA (11, 14, 15). The roles of MbnB and MbnC could not be separately determined as attempts to separately purify these gene products in *E. coli* failed (11). From these data, it has been argued that MbnBC must act in concert and by doing so create both heterocyclic groups in MBs (11). Such conclusions, however, appear to be premature for several reasons. First, the reported spectra (11) only show the presence of the C-terminal oxazolone group, not the N-terminal oxazolone group, as the 394-nm absorption maximum is missing. Second, the absorption maximum at 302 nm, diagnostic for the presence of the N-terminal oxazolone group, was absent (5, 8, 16). Third, no structural data were provided to support the presence of both oxazolone groups. To examine if MbnB and -C act in concert and are involved in the formation of both oxazolone groups in *M. trichosporium* OB3b, an MbnC deletion mutant ($\Delta mbnC$) was constructed. The results show MbnC is required for the formation of the C-terminal oxazolone group, but not for the formation of the N-terminal oxazolone group.

RESULTS

Generation of the $\Delta mbnC$ mutant. The previously constructed $\Delta mbnAN$ strain, whereby the *mbnABCMN* genes were deleted using a sucrose counterselection technique (9), was back complemented with *mbnABMN* through selective amplification and ligation of *mbnAB* with *mbnMN*, deleting *mbnC*, and inserting this ligation product into pTJS140, creating pWG104 (Table 1). Successful removal of *mbnC* from this product was confirmed via sequencing (data not shown). The native σ^{70} -dependent promoter upstream of *mbnA* was also incorporated into pWG104, and expression of *mbnABMN* but not *mbnC* (from pWG104), as well as *mbnPH* (from the chromosome) was confirmed via reverse transcription-PCR (RT-PCR) (see Fig. S1 and S2 in the supplemental material).

UV-visible absorption and mass spectrometry of metal-free MB from *M. trichosporium* OB3b $\Delta mbnC$. Comparison of the UV-visible absorption spectra of MB from *M. trichosporium* OB3b $\Delta mbnC$ to wild-type MB-OB3b suggested the presence of the N-terminal oxazolone group, but the absence of C-terminal oxazolone (Fig. 1: see Fig. S3 in the supplemental material). The molecular mass of native, full-length MB-OB3b is 1,154 Da, and that of MB-OB3b lacking the C-terminal Met is 1,023 Da. It should be noted that both forms of MB-OB3b are present in most MB-OB3b preparations (2, 5, 17). The molecular mass of $\Delta MbnC$ was 1,024 as determined by matrix-assisted laser desorption ionization-time of flight (MALDI-TOF) mass spectrometry (MS) (Fig. 2) (9), which was within 1 Da of the predicted molecular mass of MB-OB3b, in which only one oxazolone group was formed. Taken together, the UV-visible absorption spectra and molecular mass data suggest the $\Delta mbnC$ mutant lacked the C-terminal Met as well as the N-terminal oxazolone group with a 1-(N-[mercapto-(5-oxo-2-(3-methylbutanoyl)oxazol-(Z)-4-ylidene)methyl]-GSCYPCSC predicted structure (Fig. 3B). In contrast to wild-type MB-OB3b, the C-terminal Met was never observed in MbnC.

TABLE 1 Strains, plasmids, and primers used in this study

Strain, plasmid, or primer	Description ^a	Restriction site	Reference or source
Strains			
<i>Escherichia coli</i>			
TOP10	F ⁻ <i>mcrA</i> Δ(<i>mrr-hsdRMS-mcrBC</i>) φ80 <i>lacZ</i> ΔM15 Δ <i>lacX74</i> <i>recA1</i> <i>araD139</i> Δ(<i>ara leu</i>)7697 <i>galU</i> <i>galk</i> <i>rpsL</i> (Str ^r) <i>endA1</i> <i>nupG</i>		Invitrogen
S17-1 λ <i>pir</i>	<i>recA1</i> <i>thi</i> <i>pro</i> <i>hsdR</i> mutant RP4-2Tc::Mu Km::Tn7 λ <i>pir</i>		26
<i>Methylosinus trichosporium</i>			
OB3b	Wild-type strain		
Δ <i>mbnAN</i> mutant	<i>mbnABC</i> deleted		9
Δ <i>mbnC</i> mutant	Δ <i>mbnAN</i> carrying pWG104		this study
Plasmids			
pTJS140	Broad-host-range cloning vector; Mob Ap' Sp' Sm' <i>lacZ</i>		34
pWG104	pTJS140 carrying <i>mbnABC</i> with its native promoter		This study
Primers			
<i>mbnAN</i> _F	<u>ATTTTT</u> ggtaccGACGTTCCGGTCTTCTTCGC	KpnI	9
<i>mbnAN</i> _R	ATTTTT <u>ggtacc</u> CGCTCTAGATCATTCCGAC	KpnI	9
<i>mbn66</i>	<u>ATTTTT</u> ggtaccCGAACAAATGTGTGCCAGTAG	BamHI	This study
<i>mbn70</i>	<u>ATTTTT</u> ggtaccGTTCCGGCTATTTCTGACGC	BamHI	This study
<i>qmbnA</i> _{FO}	TGGAAACTCCCTTAGGAGGAA		35
<i>qmbnA</i> _{RO}	CTGCACGGATAGCACGAAC		35
<i>qmbnB</i> _{F1}	TGGTCCAGCAGATGATCAAAG		This study
<i>qmbnB</i> _{R2}	TTCCCAGCTTCTCCAATTC		This study
<i>dmbnC</i> _F	GGGAGAACAACTCGCTTT		This study
<i>dmbnC</i> _R	CTTCCCAGCAGATCTGAC		This study
<i>qmbnM</i> _F	GCTAGGCTGGCTCCTTTATC		This study
<i>qmbnM</i> _R	GATGTTGACCACAAACCGAAAG		This study
<i>qmbnN</i> _F	CGATTCCATCCTTTCCGATGT		This study
<i>qmbnN</i> _R	CACTTTGAAGACAAGGAGAGA		This study
<i>qmbnP</i> _F	AAAGGGAAGCACACCCCAT		This study
<i>qmbnP</i> _R	GTCGTGTTCTTGGCCGGATT		This study
<i>qmbnH</i> _F	ACTTACCGAAATACATCCCGC		This study
<i>qmbnH</i> _R	CGGAGAGGCGCTTATCGTAG		This study

^aAdded overhangs for binding by restriction enzyme are underlined. Restriction sites are noted with lowercase letters.

Chemical structure of metal-free Δ*mbnC* mutant as determined by NMR spectroscopy.

Metal-free MB has multiple conformations, making structural studies of MBs via solution nuclear magnetic resonance (NMR) or crystallography difficult (see Fig. S4 in the supplemental material). In prior structural studies of MB, the addition of Cu²⁺ (which is bound and reduced to Cu¹⁺ by native MB-OB3b) stabilizes MB-OB3b into one conformation, allowing for crystal formation and NMR characterization (Fig. S4) (2–5, 8, 18). Our initial efforts to investigate the structure of the MB intermediate produced by the Δ*mbnC* strain via NMR were unsuccessful.

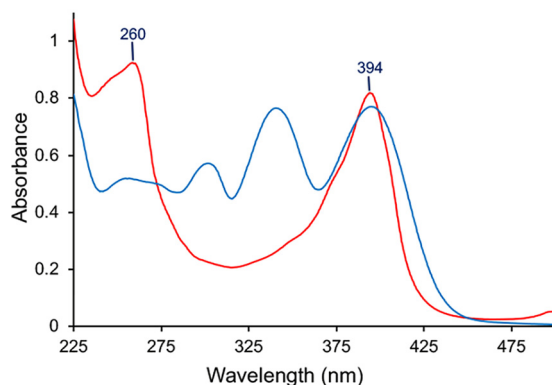


FIG 1 UV-visible absorption spectra of MB-OB3b (blue) and the Δ*mbnC* mutant (red). Abbreviations: OxaA, oxazolone A or the N-terminal oxazolone group; OxaB, oxazolone B or the C-terminal oxazolone group.

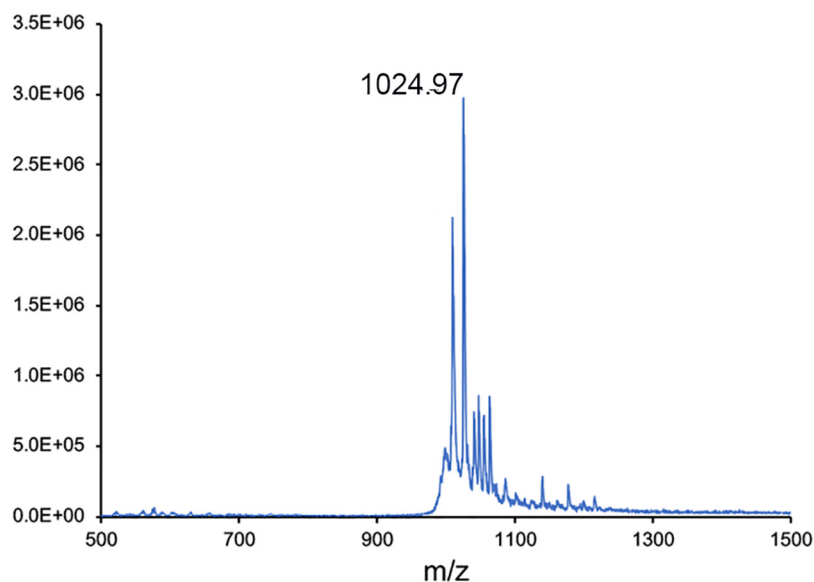


FIG 2 MALDI-TOF MS of methanobactin from $\Delta mbnC$.

In contrast to native MB, the MB intermediate from the $\Delta mbnC$ strain bound, but did not reduce Cu^{2+} to Cu^+ , resulting in peak broadening from paramagnetic Cu^{2+} . This necessitated a different strategy. Substituting other metals with similar binding behavior for copper such as Au^{3+} , Zn^{2+} , Co^{2+} , and Ni^{2+} also failed to produce well-behaved complexes. Therefore, it was necessary to examine the metal-free $\Delta mbnC$ mutant.

At standard temperature and pressure, the $\Delta mbnC$ mutant undergoes exchange between multiple conformations on an intermediate time scale, leading to excessive line broadening (see Fig. S5 in the supplemental material). In order to slow down the rate of exchange and reduce line broadening, we sampled various temperature and hydrostatic pressure conditions. We found that two-dimensional (2D) ^1H - ^{15}N NMR spectra of the $\Delta mbnC$ mutant recorded at high pressure (300,000,000 Pa) and low temperature (265 K) (18, 19) show significantly reduced line broadening and gave excellent spectra in the absence of copper (Fig. 4).

A series of NMR experiments were conducted on the $\Delta mbnC$ mutant, including homonuclear correlation spectroscopy (COSY), total correlation spectroscopy (TOCSY), rotating-frame

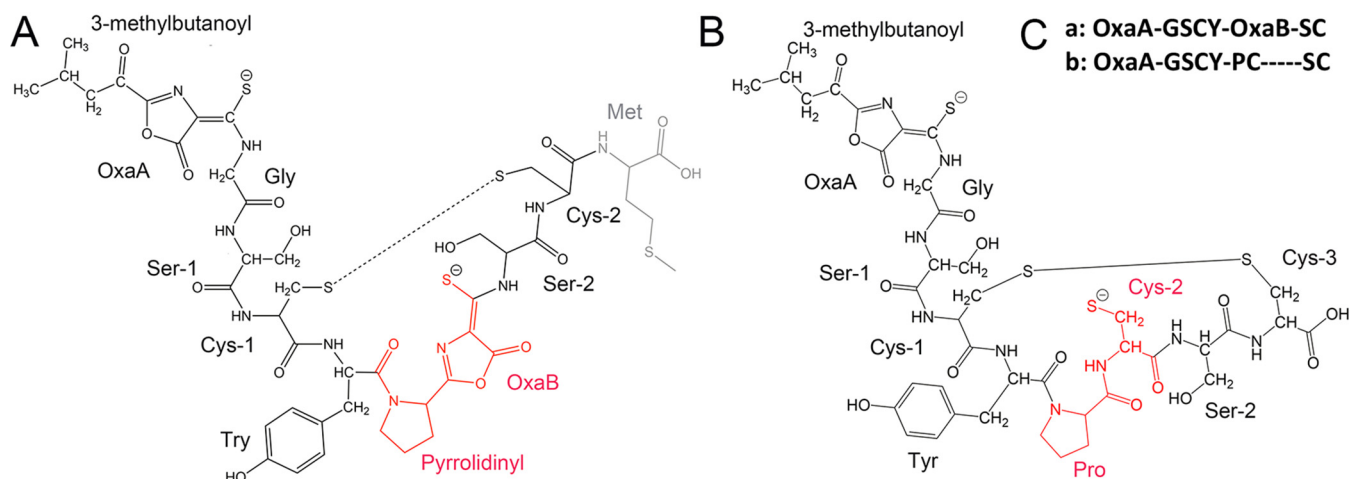


FIG 3 (A) Structure of wild-type MB-OB3b, with the labile terminal methionine in gray. (B) Proposed structure of the $\Delta mbnC$ mutant based on UV-visible absorption spectra, LC-MS, and NMR analysis. The differences between MB-OB3b-Met and the $\Delta mbnC$ mutant are highlighted in red. (C) Amino acid sequence of (a) wild-type MB-OB3b minus the C-terminal Met and (b) the $\Delta mbnC$ mutant.

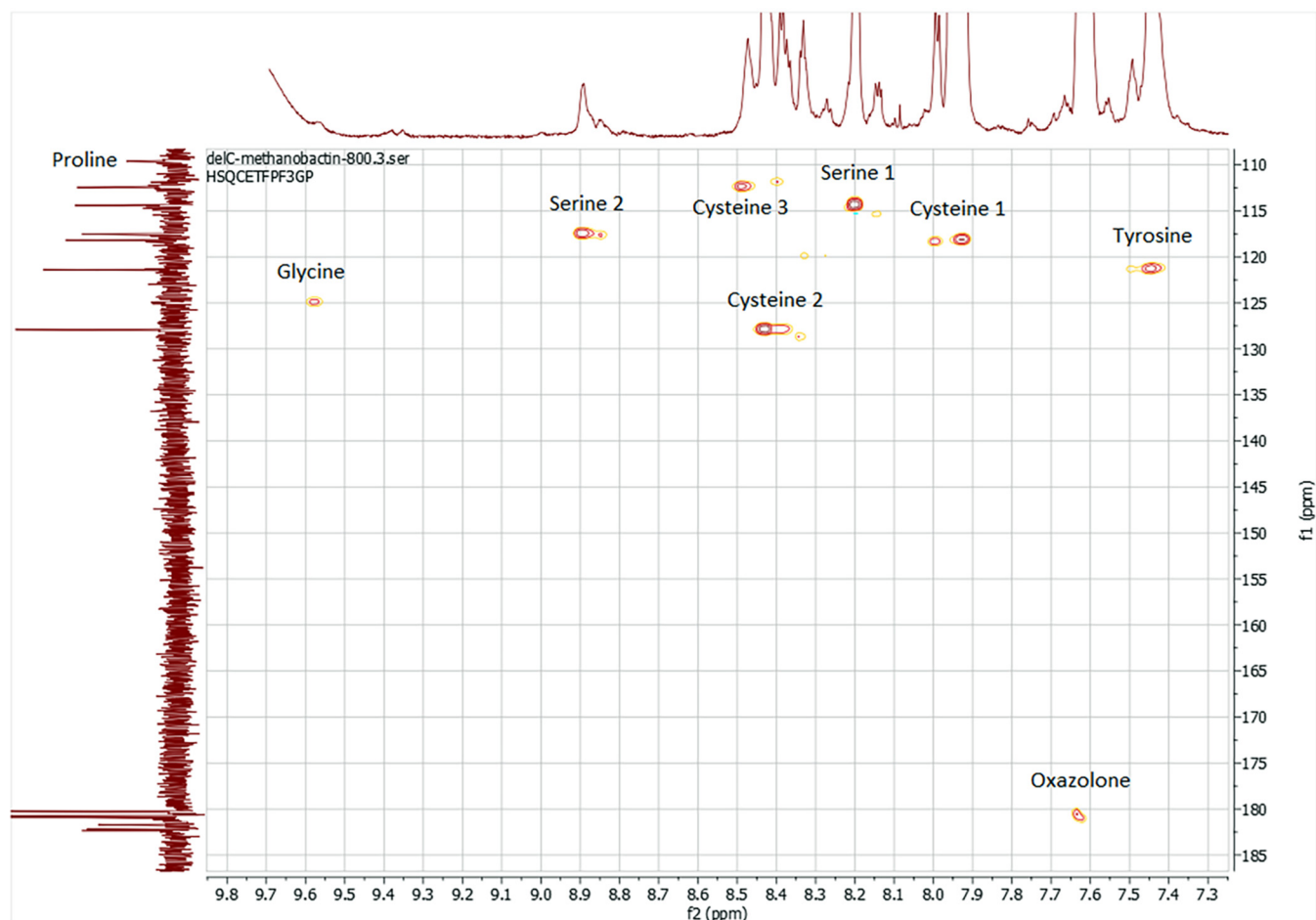


FIG 4 The 800-MHz ^1H - ^{15}N -HSQC spectrum of uniformly ^{15}N -labeled ΔmbnC mutant in 90% 9 mM phosphate buffer (pH 6.5) and 10% D_2O at 265 K and 300,000,000 Pa. The horizontal and vertical 1D spectra are ^1H and ^{15}N spectra, respectively.

nuclear Overhauser effect spectroscopy (ROESY), ^1H - ^{15}N and ^1H - ^{13}C heteronuclear single-quantum correlation spectroscopy (HSQC), and heteronuclear multiple-bond correlation spectroscopy (HMBC). These experiments enabled assigning all nonhydroxyl ^1H , nonconjugated ^{13}C , and all ^{15}N resonances (Table 2 and Fig. 4; see Fig. S6 in the supplemental material). The assigned chemical shifts show that the MB from the ΔmbnC mutant contains 8 amino acids—3 Cys, 2 Ser, 1 Gly, 1 Tyr and 1 Pro—and 1 oxazolone group (Fig. 4). The 1D ^{15}N experiment showed a peak at 109 ppm that was absent from the ^1H - ^{15}N HSQC spectra and was assigned to proline. However, the glycine nitrogen peak was especially broad, and could only be assigned with the ^1H - ^{15}N HSQC. Finally, while the 1D ^{15}N experiment had several resonances around 180 ppm—likely due to hydrolysis and deprotonation—only one of them had a correlation with ^1H in the ^1H - ^{15}N HSQC, indicating a single oxazolone group. The NMR results are consistent with the UV-visible absorption spectra and the ESI MS results, as well as with the structure shown in Fig. 3B.

DISCUSSION

Due to the variability in the core sequences of structurally characterized MBs, it is difficult to use *mbnA* to screen the potential ability of microbes to produce MB. Instead, *mbnB* and *mbnC* sequences are commonly used as they are found in all known *mbn* gene clusters (5, 13). All known MBs contain two heterocyclic rings, with the N-terminal ring found to be either an oxazolone, pyrazinedione, or imidazolone ring, while the C-terminal ring was always found to be an oxazolone. Given these data, it could be presumed that MbnBC is involved in the formation of the C-terminal oxazolone group along with an associated

TABLE 2 ^1H , ^{13}C , and ^{15}N resonances for metal-free ΔmbnC mutant^a

Residue	Atom	Chemical shift (ppm)			Residue	Atom	Chemical shift (ppm)		
		^1H	^{13}C	^{15}N			^1H	^{13}C	^{15}N
3-Methyl-butanoyl	C ¹		174.6		Tyr ⁴	H ^N	7.44		
	C ²		50.5			H ^α	2.96		
	C ³		38.0			H ^β	2.79		
	C ⁴		19.6			H ^β	1.20		
	C ⁵		19.6			H ^{2,6}	6.11		
	H ²	4.15				H ^{3,5}	6.45		
	H ³	2.17			Pro ⁵	N ¹			109.6
	H ³	2.72				C ²		67.3	
	H ⁴	1.88				C ³		21.1	
	H ⁵	1.80			C ⁴		39.5		
Oxazolone	N			180.1		C ⁵		55.2	
	H ^N	7.61				H ²	3.67		
Gly ¹	N			125.1		H ³	1.06		
	C					H ³	2.13		
	C ^α		26.6			H ⁴	1.28		
	H ^N	9.57				H ⁴	2.29		
	H ^α	1.46				H ⁵	2.79		
Ser ²	N			114.3		H ⁵	2.96		
	C		181.6		Cys ⁶	N			127.9
	C ^α		72			C		136.3	
	C ^β					C ^α		53.3	
	H ^N	8.19				C ^β		49.3	
	H ^α	4.14				H ^N	8.43		
	H ^β	3.98				H ^α	3.96		
	H ^β	1.41				H ^β	3.23		
Cys ³	N			118.1		H ^β	1.38		
	C		173.0		Ser ⁷	N			117.5
	C ^α		71.2			C			
	C ^β		35.6			C ^α		51.6	
	H ^N	7.93				C ^β		45.0	
	H ^α	3.96				H ^N	8.90		
	H ^β	3.23				H ^α	4.19		
		H ^β	1.37				H ^β	3.25	
Tyr ⁴	N			121.5		H ^β	1.48		
	C				Cys ⁸	N			112.4
	C ^α		48.9			C		172.6	
	C ^β		35.6			C ^α		42.3	
	C ¹					C ^β		21.1	
	C ^{2,6}					H ^N	8.47		
	C ^{3,5}		135.4			H ^α	3.69		
		C ⁴					H ^β	3.55	
						H ^β	0.97		

^aThe table is presented in a two-column format (i.e., the table's two "Residue" columns and corresponding data are independent from one another).

thioamide, while the N-terminal oxazolone group is formed via a different process, such as the involvement of an aminotransferase, as concluded earlier (5, 9, 10, 13).

Other researchers have attempted to elucidate the role of MbnB and MbnC in methanobactin maturation (11). These individuals were unable to separately heterologously express soluble protein from either MbnB or MbnC, but were able to coheterologously express MbnC as a heterodimeric complex. In studies where the MbnA precursor polypeptide was incubated with this MbnBC complex, the authors conclude that MbnBC was involved in the formation of both oxazolone groups and the associated thioamides of MB-OB3b. It should be noted, however, that in this study, no structural evidence (i.e., solution NMR data) was provided to definitively show the presence of

either ring; rather, such conclusions were largely based on mass spectral analyses of MbnA after incubation with the MbnBC complex. Further, the authors assumed that since their construct did not contain the N-terminal aminotransferase MbnN, the extended conjugation resulting from this reaction would result in both oxazolone groups having identical absorption maxima. The idea that the extended conjugation of the N-terminal oxazolone could be responsible for the bathochromic shift was first proposed as a possible reason for the 50-nm shift in the absorption maxima by Krentz et al. (5). Kenney et al. used this theory to bolster their claim that both oxazolone groups were present in the product from their heterologous system, with both oxazolone groups showing identical absorption spectra (11). The evidence to support this claim came from their *M. trichosporium* OB3b $\Delta mbnN$ strain. MbnN is responsible for the deamination of the N-terminal Leu in *M. trichosporium* OB3b, extending the conjugation one additional double bond. In this study, the authors claim they can stabilize the MB produced by the $\Delta mbnN$ strain by the addition of copper before purification. UV-visible absorption spectra of copper-containing $\Delta mbnN$ mutant suggest the possible presence of two oxazolone groups but no additional evidence was provided supporting this claim.

This observation was surprising as the MB produced by the $\Delta mbnN$ strain in our laboratory showed similar UV-visible absorption spectra throughout the growth cycle, suggesting the absence of the N-terminal oxazolone group (see Fig. S7 in the supplemental material). In addition, the UV-visible absorption spectra, liquid chromatography (LC)-MS/MS, Fourier transform ion cyclotron resonance (FT-ICR) MS, amino acid analysis, number of thiol groups, copper-binding properties, and pattern of acid hydrolysis demonstrate the absence of the N-terminal oxazolone group in the $\Delta mbnN$ mutant (9).

Additional evidence that the bathochromic shift in MBs with two oxazolone groups is unlikely to solely arise from the addition of one double bond following deamination of the N-terminal amine comes from examination of the group I MB from *Methylocystis parvus* OBBP. Acid hydrolysis of the MB from *M. parvus* OBBP shows a similar hydrolysis pattern to that observed with the MB from *M. trichosporium* OB3b, demonstrating the presence of two oxazolone groups, with absorption maxima at 340 and 390 nm (see Fig. S8 in the supplemental material). However, both MB operons from *M. parvus* OBBP lack *mbnN*, and without deamination of the N-terminal Phe, the conjugation around the N-terminal oxazolone group would not be extended. It is possible that another aminotransferase in the *M. parvus* OBBP genome may catalyze deamination of the N-terminal Phe. However, this appears unlikely as deamination of the N-terminal amino acid has never been observed in structurally characterized MBs from operons lacking *mbnN* (3, 5). The results suggest deamination of the N-terminal amino acid is not solely responsible for the 40- to 50-nm absorption maximum difference between oxazolone groups in MBs. The absence of either the N-terminal or C-terminal oxazolone group in a small (0.5 to 2%) fraction of most MB-OB3b preparations (Fig. S3) also questions the suggestion that the absorption maximum difference between the N-terminal and C-terminal oxazolone groups is due solely to extending the conjugation of an additional double bond introduced following the deamination reaction.

The results presented here confirm MbnC is required for the formation of the C-terminal oxazolone group (Fig. 5). However, the results presented here also demonstrate MbnC is not required for the formation of the N-terminal oxazolone group in *M. trichosporium* OB3b, suggesting the formation of the two heterocyclic groups with associated thioamides from XC dipeptides does not utilize the same enzyme(s). Future studies will determine if MbnB is involved in the formation of the N-terminal oxazolone, pyranzinedione, or imidazolone groups. Resolution of the pathway and enzymes responsible for the posttranslational modifications required for the synthesis of MB in methanotrophic bacteria will aid in the production of MB derivatives with pharmacological properties specific for different metal-related diseases (19–24) as well as for environmental applications (10, 25).

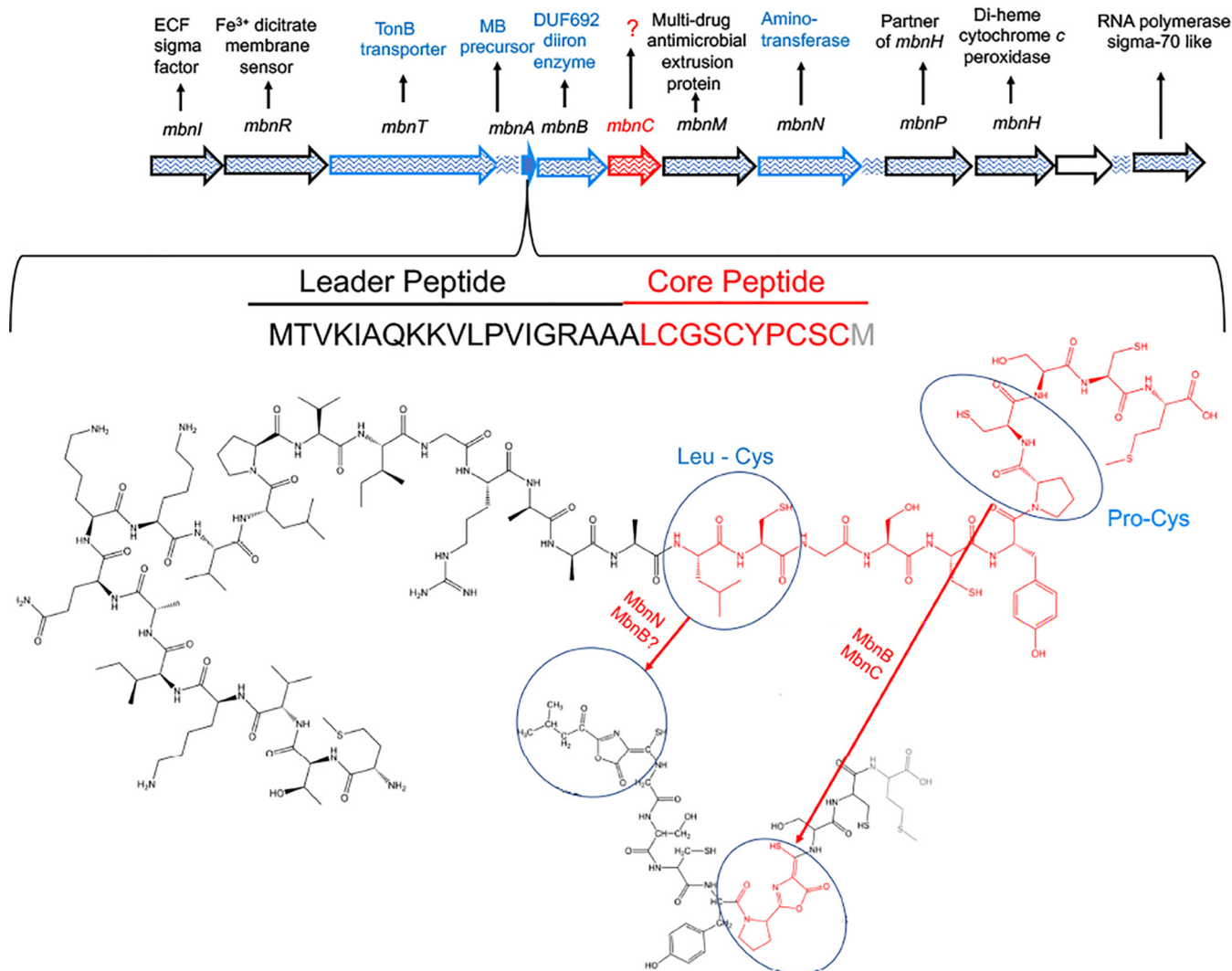


FIG 5 (Top) MB-OB3b gene cluster. Genes with known involvement in MB-OB3b synthesis and transport are shown in blue. (Bottom) Proposed genes involved in the biosynthesis of the oxazolone rings with associated thioamides from MbnA. Additional, yet to be identified genes may also be involved in the formation of oxazolone groups.

MATERIALS AND METHODS

Bacterial strains, growth media, and culture conditions. Plasmid construction was accomplished using *Escherichia coli* strain TOP10 (Invitrogen, Carlsbad, CA) as described previously (9). Plasmids used and constructed during this study are shown in Table 1. The donor strain for conjugation of plasmids into *Methylosinus trichosporium* OB3b was *E. coli* S17-1 (26). *E. coli* strains were cultivated at 37°C in Luria broth medium (Dot Scientific, Burton, MI). Methanotrophic strains (i.e., *M. trichosporium* OB3b wild type, *M. trichosporium* OB3b Δ *mbnAN*, *M. trichosporium* OB3b Δ *mbnC*, *Methylocystis* sp. strain SB2, and *Methylocystis parvus* OBBP) were cultivated at 30°C on nitrate mineral salts (NMS) medium (27), either in 250-mL flasks with side-arms at 200 rpm or in a 15-L New Brunswick Bioflow 310 fermenter (Eppendorf, Hauppauge, NY), using methane as the sole carbon and energy source. Where necessary, filter-sterilized solutions of copper (as CuCl_2) and spectinomycin were added to culture media aseptically. A working concentration of 20 $\mu\text{g mL}^{-1}$ spectinomycin was used for maintaining pWG104 in the *M. trichosporium* OB3b Δ *mbnAN* deletion mutant (i.e., *M. trichosporium* OB3b Δ *mbnC*). Chemicals were purchased from Fisher Scientific (Waltham, MA) or Sigma-Aldrich (St. Louis, MO) of American Chemical Society reagent grade or better.

For ^{15}N NMR, K^{14}NO_3 in NMS medium was replaced with K^{15}NO_3 (Cambridge Isotope Laboratories, Cambridge, MA).

General DNA methods, transformation, and conjugation. DNA purification and plasmid extraction were performed using QIAquick and QIAprep kits from Qiagen following the manufacturer's instruction. DNA cloning, preparation of chemically competent cells, and plasmid transformation with *E. coli* were performed according to reference 28. Enzymes used for restriction digestion and ligation were purchased from New England Biolabs (Ipswich, MA). PCR of DNA for cloning purposes was accomplished using iProof high-fidelity polymerase (Bio-Rad, Hercules, CA). PCR for general purposes was

accomplished using GoTaq DNA polymerase (Promega, Fitchburg, WI). PCR programs were set according to the manufacturer's suggestions. Plasmid pWG104 was conjugated into *M. trichosporium* OB3b Δ *mbnAN* with *E. coli* S17-1 as the donor strain as described by Martin and Murrell (29).

Construction of the *M. trichosporium* OB3b Δ *mbnC* strain. Previously, an *M. trichosporium* mutant was constructed in which *mbnABC MN* was deleted using a counterselection technique (9). To characterize the function of *mbnC*, a Δ *mbnC* mutant was constructed by introducing the pWG104 expression vector into the Δ *mbnAN* mutant. pWG104 was constructed by cloning two separate DNA fragments, one of which was a 1.9-kb DNA fragment of *mbnAB* (created via use of primers *mbnANf* and *mbn66*) and the other of which was a 2.5-kb DNA fragment of *mbnMN* (created via use of primers *mbn70* and *mbnANr*), leaving out *mbnC*. These two fragments were amplified with BamHI restriction sites as indicated in Fig. S2. These were then ligated together and cloned into the broad-host-range vector pTJS140 at the KpnI site.

Extraction of RNA and RT-PCR. To check the expression of genes restored to the *M. trichosporium* OB3b Δ *mbnC* mutant (e.g., *mbnA*, *-B*, *-M*, and *N*), genes associated with MB remaining in the chromosome (*mbnPH*), as well as the absence of *mbnC*, RNA from the Δ *mbnC* mutant was collected, purified, and reverse transcribed to cDNA to perform RT-PCR. Total RNA was isolated as described earlier (9). Briefly, the Δ *mbnC* mutant was grown to the exponential phase, and RNA was extracted using a phenol-chloroform method modified from Griffiths et al. (30). Collected RNA was purified and removal of DNA confirmed by the absence of 16S rRNA PCR product from PCRs. The same amount of RNA (500 ng) was used for reverse transcription by SuperScript III reverse transcriptase (Invitrogen, Carlsbad, CA) for all reactions. RT-PCR analyses were performed to confirm the expression of *mbnABMNPH* as well as the absence of *mbnC* using primers listed in Table 1.

Isolation of MB from *M. trichosporium* OB3b, *Methylocystis* strain SB2, *Methylocystis parvus* OBBP, and the Δ *mbnC* mutant. MBs from all three methanotrophs were purified as previously described (31).

UV-visible absorption spectra. UV-visible absorption spectra of MbnC⁻ high-performance liquid chromatography (HPLC) fractions from MB preparations from *M. trichosporium* OB3b and *Methylocystis* strain SB2 and from the MB from *M. parvus* OBBP were determined as previously described (32, 33). Acid hydrolysis of the oxazolone groups in the MB from *M. parvus* OBBP was carried out in 85 μ M acetic acid as previously described (32).

Structural characterization of the Δ *mbnC* mutant. UV-visible spectroscopy was recorded on a Cary 50 spectrometer (Agilent, Santa Clara, CA). Matrix-assisted laser desorption ionization-time of flight (MALDI-TOF) MS was performed on a Shimadzu AXIMA Confidence MALDI-TOF mass spectrometer (Shimadzu, Kyoto, Japan). Samples resuspended in 20 mM Tris-HCl buffer, pH 8.0 (10 to 20 μ g \cdot μ l⁻¹), were mixed in a 1:1 ratio with matrix Super dihydroxybenzoic acid (Super DHB), and 1 μ l of this mixture was loaded on a DE1580TA plate (from Shimadzu) and allowed to dry at room temperature. Super DHB was prepared from 9 parts 2,5-dihydroxybenzoic acid (DHB) and 1 part 2-hydroxy-5-methoxybenzoic acid (Sigma-Aldrich, St. Louis, MO), both prepared in 70% acetonitrile–29.9% H₂O–0.1% trifluoroacetic acid. NMR experiments were performed on a Bruker Advance 700 (Bruker, Allentown, PA) with a Bruker 5-mm TCI 700 H/C/N cryoprobe or on a Bruker Advance 800 with a Bruker 5-mm TCI 800 H/C/N cryoprobe. NMR solutions were made using 15 to 40 mg uniformly ¹⁵N-MB-OB3b in a 90:10 H₂O-D₂O mixture at pH 6.5. Unless otherwise specified, all experiments were run at 265 K and 300,000,000 Pa. Samples were placed in 300,000,000-Pa-rated sapphire NMR tubes (Daedalus Innovations, LLC, Beaverdam, VA), and high pressure was generated by an Xtreme 60 (Daedalus Innovations). Analysis was performed in Mnova (Mestrelab Research, Escondido, CA).

SUPPLEMENTAL MATERIAL

Supplemental material is available online only.

SUPPLEMENTAL FILE 1, PDF file, 1.8 MB.

ACKNOWLEDGMENTS

This research was supported by the U.S. Department of Energy Office of Science (grants DE-SC0018059 and DE-SC0020174 to J.D.S. and A.A.D.), the National Science Foundation (grant 1912482 to J.D.S.), the Roy J. Carver Charitable Trust (Muscatine, IA, USA) (to J.R.), and an ISU Bailey Research and Career Development award (to T.A.B.). Use of the Bruker Advance 800 was made possible through a generous gift from the Roy J. Carver Charitable Trust.

We declare no conflict of interest.

REFERENCES

- DiSpirito AA, Semrau JD, Murrell JC, Gallagher WH, Dennison C, Vuilleumier S. 2016. Methanobactin and the link between copper and bacterial methane oxidation. *Microbiol Mol Biol Rev* 80:387–409. <https://doi.org/10.1128/MMBR.00058-15>.
- El Ghazouani A, Basle A, Firbank SJ, Knapp CW, Gray J, Graham DW, Dennison C. 2011. Copper-binding properties and structures of methanobactins from *Methylosinus trichosporium* OB3b. *Inorg Chem* 50:1378–1391. <https://doi.org/10.1021/ic101965j>.
- El Ghazouani A, Basle A, Gray J, Graham DW, Firbank SJ, Dennison C. 2012. Variations in methanobactin structure influences copper utilization by methane-oxidizing bacteria. *Proc Natl Acad Sci U S A* 109:8400–8404. <https://doi.org/10.1073/pnas.1112921109>.
- Kim HJ, Graham DW, DiSpirito AA, Alterman MA, Galeva N, Larive CK, Asunskis D, Sherwood PM. 2004. Methanobactin, a copper-acquisition compound from methane-oxidizing bacteria. *Science* 305:1612–1615. <https://doi.org/10.1126/science.1098322>.

5. Krentz BD, Mulheron HJ, Semrau JD, DiSpirito AA, Bandow NL, Haft DH, Vuilleumier S, Murrell JC, McEllistrem MT, Hartsel SC, Gallagher WH. 2010. A comparison of methanobactins from *Methylosinus trichosporium* OB3b and *Methylocystis* strain SB2 predicts methanobactins are synthesized from diverse peptide precursors modified to create a common core for binding and reducing copper ions. *Biochemistry* 49:10117–10130. <https://doi.org/10.1021/bi1014375>.
6. Semrau JD, DiSpirito AA, Obulisamy PK, Kang CS. 2020. Methanobactin from methanotrophs: genetics, structure, function and potential applications. *FEMS Microbiol Lett* 367:feaa045.
7. Semrau JD, DiSpirito AA, Gu W, Yoon S. 2018. Metals and methanotrophy. *Appl Environ Microbiol* 84:e02289-17. <https://doi.org/10.1128/AEM.02289-17>.
8. Behling LA, Hartsel SC, Lewis DE, DiSpirito AA, Choi DW, Masterson LR, Veglia G, Gallagher WH. 2008. NMR, mass spectrometry and chemical evidence reveal a different chemical structure for methanobactin that contains oxazolone rings. *J Am Chem Soc* 130:12604–12605. <https://doi.org/10.1021/ja804747d>.
9. Gu W, Baral BS, DiSpirito AA, Semrau JD. 2017. An aminotransferase is responsible for the deamination of the N-terminal leucine and required for formation of oxazolone ring A in methanobactin of *Methylosinus trichosporium* OB3b. *Appl Environ Microbiol* 83:e02619-16. <https://doi.org/10.1128/AEM.02619-16>.
10. Semrau JD, DiSpirito AA, Obulisamy PK, Kang-Yun CS. 2020. Methanobactin from methanotrophs: genetics, structure, function and potential applications. *FEMS Microbiol Lett* 367:fnaa045. <https://doi.org/10.1093/femsle/fnaa045>.
11. Kenney GE, Dassama LMK, Pandelia M-E, Gizzi AS, Martinie RJ, Gao P, DeHart CJ, Schachner LF, Skinner OS, Ro SY, Zhu X, Sadek M, Thomas PM, Almo SC, Bollinger MJ, Krebs C, Kelleher NL, Rosenzweig AC. 2018. The biosynthesis of methanobactin. *Science* 359:1411–1416. <https://doi.org/10.1126/science.aap9437>.
12. Gu W, Farhan UI Haque M, Baral BS, Turpin EA, Bandow NL, Kremmer E, Flatley A, Zischka H, DiSpirito AA, Semrau JD. 2016. A TonB dependent transporter is responsible for methanobactin uptake by *Methylosinus trichosporium* OB3b. *Appl Environ Microbiol* 82:1917–1923. <https://doi.org/10.1128/AEM.03884-15>.
13. Kenney GE, Rosenzweig AC. 2013. Genome mining for methanobactins. *BMC Biol* 11:17. <https://doi.org/10.1186/1741-7007-11-17>.
14. Chou JC-C, Strafford VE, Kenney GE, Dassama LMK. 2021. The enzymology of oxazolone and thioamide synthesis in methanobactin. *Methods Enzymol* 656: 341–373. <https://doi.org/10.1016/bs.mie.2021.04.008>.
15. Choi DW, Do YS, Zea CJ, McEllistrem MT, Lee SW, Semrau JD, Pohl NL, Kisting CJ, Scardino LL, Hartsel SC, Boyd ES, Geesey GG, Riedel TP, Shafe PH, Kranski KA, Tritsch JR, Antholine WE, DiSpirito AA. 2006. Spectral and thermodynamic properties of Ag(I), Au(III), Cd(II), Co(II), Fe(III), Hg(II), Mn(II), Ni(II), Pb(II), U(IV), and Zn(II) binding by methanobactin from *Methylosinus trichosporium* OB3b. *J Inorg Biochem* 100:2150–2161. <https://doi.org/10.1016/j.jinorgbio.2006.08.017>.
16. Eckert P, Johs A, Semrau JD, DiSpirito AA, Richardson J, Sarangi R, Herndon E, Gu B, Pierce EM. 2021. Spectroscopic and computational investigations of organometallic complexation of group 12 transition metals by methanobactins from *Methylocystis* sp. SB2. *J Inorg Biochem* 223:111496. <https://doi.org/10.1016/j.jinorgbio.2021.111496>.
17. Bandow NL, Gallagher WH, Behling L, Choi DW, Semrau JD, Hartsel SC, Gilles VS, DiSpirito AA. 2011. Isolation of methanobactin from the spent media of methane-oxidizing bacteria. *Methods Enzymol* 495:259–269. <https://doi.org/10.1016/B978-0-12-386905-0.00017-6>.
18. Kenney GE, Goering AW, Ross MO, DeHart CJ, Thomas PM, Hoffman BM, Kelleher NL, Rosenzweig AC. 2016. Characterization of methanobactin from *Methylosinus* sp. SW4. *J Am Chem Soc* 138:11124–11127. <https://doi.org/10.1021/jacs.6b06821>.
19. Zischka H, Lichtmannegger J, DiSpirito AA, Semrau JD. 2017. Means and methods of treating copper-related diseases. World patent WO2017103094A2.
20. Zischka H, Lichtmannegger J, Schmitt S, Jagemann N, Schulz S, Wartini D, Jennen L, Rust C, Larochette N, Galluzzi L, Chajes V, Bandow N, Gilles VS, DiSpirito AA, Esposito I, Goettlicher M, Summer KH, Kroemer G. 2011. Liver mitochondrial membrane crosslinking and destruction in a rat model of Wilson disease. *J Clin Invest* 121:1508–1518. <https://doi.org/10.1172/JCI45401>.
21. Lichtmannegger J, Leitzinger C, Wimmer R, Schmitt S, Schulz S, Kabiri Y, Eberhagen C, Rieder T, Janik D, Neff F, Straub BK, Schirmacher P, DiSpirito AA, Bandow N, Baral BS, Flatley A, Kremmer E, Denk G, Reiter FP, Hohenester S, Eckardt-Schupp F, Dencher NA, Adamski J, Sauer V, Niemiets C, Schmidt HHJ, Merle U, Gotthardt DN, Kroemer G, Weiss KH, Zischka H. 2016. Methanobactin: a new effective treatment strategy against acute liver failure in a Wilson disease rat model. *J Clin Invest* 126:2721–2735. <https://doi.org/10.1172/JCI85226>.
22. Choi DW, Semrau JD, Antholine WE, Hartsel SC, Anderson RC, Carey JN, Dreis AM, Kenseth EM, Renstrom JM, Scardino LL, Van Gorden GS, Volkert AA, Wingad AD, Yanzer PJ, McEllistrem MT, de la Mora AM, DiSpirito AA. 2008. Oxidase, superoxide dismutase, and hydrogen peroxide reductase activities of methanobactin from types I and II methanotrophs. *J Inorg Biochem* 102:1571–1580. <https://doi.org/10.1016/j.jinorgbio.2008.02.003>.
23. Summer KH, Lichtmannegger J, Bandow N, Choi DW, DiSpirito AA, Michalke B. 2011. The biogenic methanobactin is an effective chelator for copper in a rat model for Wilson disease. *J Trace Elem Med Biol* 25:36–41. <https://doi.org/10.1016/j.jtemb.2010.12.002>.
24. Müller J-C, Lichtmannegger J, Zischka H, Sperling M, Karst U. 2018. High spatial resolution of LA-ICP-MS demonstrates massive liver copper depletion in Wilson disease rats upon methanobactin treatment. *J Trace Elem Med Biol* 49:119–127. <https://doi.org/10.1016/j.jtemb.2018.05.009>.
25. Lu X, Gu W, Zhao L, Fagan UHM, DiSpirito AA, Semrau JD, Gu B. 2017. Methylmercury uptake and degradation by methanotrophs. *Science Adv* 3:e1700041. <https://doi.org/10.1126/sciadv.1700041>.
26. Simon R. 1984. High frequency mobilization of Gram-negative bacterial replicons by the in vitro constructed Tn5-Mob transposon. *Mol Gen Genet* 196:413–420. <https://doi.org/10.1007/BF00436188>.
27. Whittenbury R, Phillips KC, Wilkinson JF. 1970. Enrichment, isolation and some properties of methane-utilizing bacteria. *J Gen Microbiol* 61:205–218. <https://doi.org/10.1099/00221287-61-2-205>.
28. Sambrook J, Russell DW. 2001. *Molecular cloning: a laboratory manual*, 3rd ed. Cold Spring Harbor Laboratory Press, Cold Spring Harbor, NY.
29. Martin H, Murrell JC. 1995. Methane monooxygenase mutants of *Methylosinus trichosporium* constructed by marker-exchange mutagenesis. *FEMS Lett* 127: 243–248. <https://doi.org/10.1111/j.1574-6968.1995.tb07480.x>.
30. Griffiths RI, Whiteley AS, O'Donnell AG, Bailey MJ. 2000. Rapid method for coextraction of DNA and RNA from natural environments for analysis of ribosomal DNA- and rRNA-based microbial community composition. *Appl Environ Microbiol* 66:5488–5491. <https://doi.org/10.1128/AEM.66.12.5488-5491.2000>.
31. Dershwitz P, Bandow NL, Yang J, Semrau JD, McEllistrem MT, Heinze RA, Fonseca M, Ledesma JC, Jennett JR, DiSpirito AA, Athwal NS, Hargrove MS, Bobik TA, Zischka H, DiSpirito AA. 2021. Oxygen generation via water splitting by a novel biogenic metal ion binding compound. *Appl Environ Microbiol* 87:e00286-21. <https://doi.org/10.1128/AEM.00286-21>.
32. Bandow N, Gilles VS, Freese-meier B, Semrau JD, Krentz B, Gallaghe W, McEllistrem MT, Hartsel SC, Cho DW, Hargrove MS, Heard TM, Chesner LM, Braunreiter KM, Cao BV, Gavitt MM, Hoopes JZ, Johnson JM, Polster EM, Schoenick BD, Am U, DiSpirito AA. 2012. Spectral and copper binding properties of methanobactin from the facultative methanotroph *Methylocystis* strain SB2. *J Inorg Biochem* 110:72–82. <https://doi.org/10.1016/j.jinorgbio.2012.02.002>.
33. Choi DW, Zea CJ, Do YS, Semrau JD, Antholine WE, Hargrove MS, Pohl NL, Boyd ES, Geesey GG, Hartsel SC, Shafe PH, McEllistrem MT, Kisting CJ, Campbell D, Rao V, de la Mora AM, DiSpirito AA. 2006. Spectral, kinetic, and thermodynamic properties of Cu(I) and Cu(II) binding by methanobactin from *Methylosinus trichosporium* OB3b. *Biochemistry* 45:1442–1453. <https://doi.org/10.1021/bi051815t>.
34. Smith TJ, Slade SE, Burton NP, Murrell JC, Dalton H. 2002. Improved system for engineering of the hydroxylase component of soluble methane monooxygenase. *Appl Environ Microbiol* 68:5265–5273. <https://doi.org/10.1128/AEM.68.11.5265-5273.2002>.
35. Semrau JD, Jagadevan S, DiSpirito AA, Khalifa A, Scanlan J, Bergman BH, Freese-meier BC, Baral BS, Bandow NL, Vorobeve A, Haft DH, Vuilleumier S, Murrell JC. 2013. Methanobactin and MmoD work in concert to act as the “copper switch” in methanotrophs. *Environ Microbiol* 15:3077–3086. <https://doi.org/10.1111/1462-2920.12150>.